EARTHQUAKE ENGINEERING AND STRUCTURAL DYNAMICS, VOL. 26, 1191–1208 (1997)

STABILITY OF ELEVATED LIQUID-FILLED CONICAL TANKS UNDER SEISMIC LOADING, PART I — THEORY

A. A. EL DAMATTY,[1]* R. M. KOROL AND F. A. MIRZA[2]

[1] *Department of Civil Engineering, The University of Western Ontario, London, Ontario, Canada, N6A 5B9*
[2] *Department of Civil Engineering, McMaster University, Hamilton, Ontario, Canada*

SUMMARY

Conical steel shells are widely used as water containments for elevated tanks. However, the current codes for design of water structures do not specify any procedure for handling the seismic design of such structures. In this paper, a numerical model is developed for studying the stability of liquid-filled conical tanks subjected to seismic loading. The model involves a previously formulated consistent shell element with geometric and material non-linearities included. A boundary element formulation is derived to obtain the hydrodynamic pressure resulting from both the horizontal and the vertical components of seismic motion acting on a conical tank which is prevented from rocking. The boundary element formulation leads to a fluid added-mass matrix which is incorporated with the shell element formulation to perform non-linear dynamic stability analysis of such tanks subjected to both horizontal and vertical components of ground motion. Although, the formulation was developed for conical vessels, it is general and can be easily modified to study the stability of any liquid-filled shell of revolution subjected to seismic loading. The accuracy of fluid added-mass formulation was verified by performing the free vibration analysis of liquid-filled cylindrical tanks and comparing the results to those available in the literature. © 1997 John Wiley & Sons, Ltd.

Earthquake Engng. Struct. Dyn., **26**, 1191–1208 (1997)

No. of Figures: 3. No. of Tables: 2. No. of References: 21.

KEY WORDS: tanks; vessels; conical; seismic; earthquake; stability; shells; finite element; boundary element

1. INTRODUCTION

Conical steel tanks with cylindrical upper sections are widely used as containment vessels for elevated water tower structures. A typical cross-section of such an elevated conical tank is shown in Figure 1. The conical steel segment is normally welded to a steel circular plate at its bottom, with the latter anchored to a reinforced concrete slab which in turn is supported by a reinforced concrete tower. The steel vessel is normally constructed from curved panels, but welded together along circumferential and longitudinal edges.

In order to perform a seismic analysis of a liquid-filled tank, the hydrodynamic pressure developed inside the tank as a result of the seismic motion has to be evaluated. Early analytical work concerning this pressure within liquid-filled tanks was conducted by Housner.[1] In this study, the hydrodynamic pressure was divided into two components; the impulsive component resulting from the movement of the walls of the tank, and the convective component due to the surface wave developing at the top. With its walls assumed rigid, a mechanical model representing both components of the fluid's hydrodynamic pressure was developed for different shapes of the container.

Later, it was recognized that the flexibility of the walls of such tanks has an important effect on the impulsive component of the hydrodynamic pressure. As such, several numerical and analytical studies conducted on cylindrical tanks focused on the interaction between flexible walls and the contained fluid due

* Correspondence to: A. A. El Damatty, Department of Civil Engineering, The University of Western Ontario, London, Ontario, Canada N6A 5B9

CCC 0098–8847/97/121191–18$17·50

Received 23 April 1996
Revised 5 June 1997

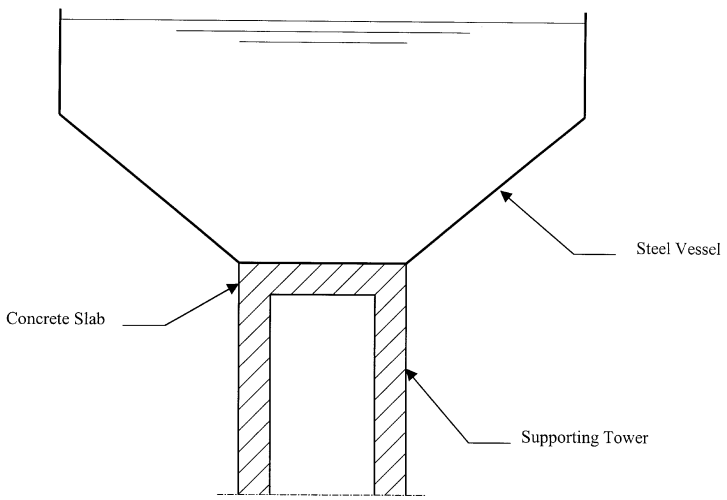

Figure 1. Cross-sectional elevation of elevated conical tanks

to the effects of horizontal ground acceleration. Major contributions were made by Velestos,[2] Balendra *et al.*,[3] Barton and Parker[4] and Haroun.[5] During this period, Haroun and Housner[6] suggested a mechanical model simulating the hydrodynamic pressure expected to develop inside a flexible cylindrical tank subjected to a horizontal excitation and prevented from rocking. The formulation was based on the boundary integral method and the fundamental mode shape of vibration of cylindrical tanks. This mechanical model was extended by Haroun and Ellaithy[7] to account for the rocking motion at the base. The effect of the vertical ground acceleration on the behaviour of liquid-filled cylinders was also investigated by Haroun and Tayel.[8,9] In these studies, the natural frequencies and the corresponding mode shapes due to axisymmetric vibrations, caused by this type of ground motion, were considered both through a closed-form analytical solution and numerically. It should be noted that all of the above studies have shown that the vibration of the tanks is affected mainly by the impulsive component of the hydrodynamic pressure.

The dynamic instability of liquid-filled cylindrical tanks under horizontal, vertical and rocking motion was more recently investigated in several studies.[10–15] In all of the above studies, dynamic stability analysis was performed using an eigenvalue approach limited to small deformation elastic response (geometric or material non-linearities were not included). Zhou *et al.*[16] further advanced the field by employing non-linear shell theory to predict the elastic buckling state of liquid storage cylindrical tanks under horizontal excitation.

To the best of the authors' knowledge, no attempt has been made to study the seismic response of liquid-filled conical tanks. In this paper, the simplification has been made to exclude the cylindrical segment characterizing most prototype structures that are in evidence in many communities. The task then has been taken to develop a numerical model which is able to simulate the seismic response of liquid-filled conical tanks and to predict the occurrence of dynamic buckling of these structures. In developing the numerical model, the following criteria were taken into account:

1. Similar to the behaviour cylindrical tanks, the flexibility of the walls of conical tanks is expected to have a significant effect on the hydrodynamic pressure developed inside the tank. As such, it was decided to use a model which indeed simulates the hydrodynamic pressure acting on flexible tanks.

2. Due to the inclination of the walls of conical tanks, the boundary conditions affecting the hydrodynamic pressure developed within are different from those acting on a cylindrical tank. As such, the mechanical model for hydrodynamic pressure which accounts for the wall flexibility of cylindrical shaped vessels cannot be used for conical tanks applications. Indeed, a formulation which simulates the interaction between the vibration of the inclined walls and the contained fluid has to be derived.
3. Again, for reasons of inclination of the walls, the vertical component of the ground acceleration will lead to both axial and hoop stresses. As such, the vertical component of the ground acceleration is expected to have a significant effect on the stability of conical tanks (compared to the case of cylindrical tanks where vertical acceleration leads only to hoop stresses) and should be included simultaneously with horizontal accelerations in the analysis.
4. Unlike cylindrical tanks, the hydrostatic pressure alone sets up both axial and hoop stresses in conical-shaped vessels, with high stress levels at the junction with its bottom plate.[17] These stresses combined with those resulting from seismic motion can lead to early yielding in the material of the tank. Therefore, the model used to simulate the seismic response of conical tanks should include the effects of material non-linearity.
5. Due to the sensitivity of thin conical shells to meridional stresses, the dynamic state of instability due to both seismic and hydrostatic loading needs to be investigated. This is accomplished numerically by modelling the walls of the tanks using shell elements which include both geometric and material non-linearities in their formulation. The inclusion of these non-linear effects will identify a tendency of local buckling which could trigger global instability. The criterion to be imposed is the vanishing of the effective stiffness of the tank. Due to the complexity associated with this problem (geometric and material non-linearities, fluid–structure interaction) the degenerated shell elements (which require only C_0 continuity) represent in our view the simplest available tool to solve this problem. Meanwhile a formulation of degenerated consistent sub-parametric shell elements used to discretize the conical shell is desirable because the spurious shear modes associated with conventional isoparametric shell elements are avoided. Such a formulation is to be applied in this investigation.

The paper starts by describing the consistent subparametric shell element. (The non-linear formulation of this element was performed and tested in a previous study given by El Damatty *et al.*[18]) This is followed by evaluation for the impulsive component of the hydrodynamic pressure developed within the cone due to both the horizontal and vertical components of ground motions using a coupled consistent shell element-boundary element formulation. This coupled formulation leads to a fluid-added mass matrix which is incorporated with the shell element formulation to investigate the state of dynamic stability of the liquid-shell system through non-linear dynamic analysis. Finally, the added-mass formulation is verified by considering the free vibration analysis of liquid-filled cylindrical tanks (as a special case of conical tanks). A companion paper (Part II) will apply the theory presented here to access the adequacy of realistic elevated conical water tower structures to seismic and gravity-type loads.

2. CONSISTENT SHELL ELEMENT

A consistent subparametric shell element was recently formulated by Koziey and Mirza.[19] The element employs cubic polynomials for approximating displacements, and, quadratic polynomials for the approximations of rotations. These functions ensure a consistent formulation and eliminate spurious shear modes and the shear locking phenomenon found to exist in isoparametric shell elements when used to model thin plates and shells. The element was derived to model thick as well as thin shell structures by including in its formulation special rotational degrees of freedom which lead to a cubic variation of the through thickness displacements (thus simulating transverse shear deformations). Since such shear deformations are probably negligible in thin conical shell structures, these special degrees of freedom were omitted in the present study.

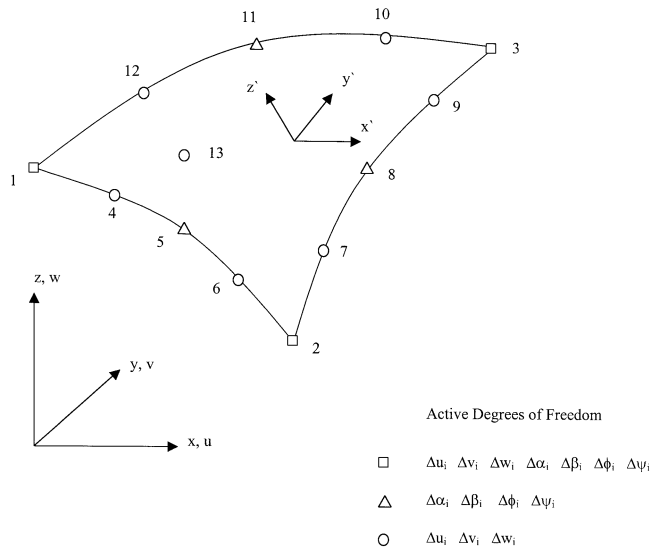

Figure 2. Consistent shell element co-ordinate systems and nodal degrees of freedom

Nonetheless, a shear correction factor 'κ' was used in the constitutive relation of the shell to account for the effect of transverse shear deformation in an average sense. As such, in the incremental formulation of the consistent shell element, the incremental displacement Δu_i is expressed using the incremental global displacement degrees of freedom ΔU_n, ΔV_n and ΔW_n directed along axes x, y and z, respectively, together with two incremental rotations $\Delta\alpha_n$ and $\Delta\beta_n$, about local axes y' and x', respectively; the latter axes are tangent to the shell mid-surface. To obtain cubic approximations for ΔU, ΔV and ΔW, the incremental displacement degrees of freedom at the corner, one-third side nodes and the centre node are used. Quadratic approximations for $\Delta\alpha$ and $\Delta\beta_n$ are achieved using the incremental rotational degrees of freedom at the corner and mid-side nodes as shown in Figure 2. The total number of degrees of freedom per element becomes 42. However, the formulation of the consistent shell element is performed by assuming that each node has all five degrees of freedom, and that the interpolation function which corresponds to a non-active degree of freedom is equal to zero.

The incremental global displacements (Δu, Δv, Δw) can now be written in terms of the nodal incremental degrees of freedom as

$$\begin{Bmatrix}\Delta u\\ \Delta v\\ \Delta w\end{Bmatrix} = \sum_{n=1}^{13} \bar{N}_n \begin{Bmatrix}\Delta U_n\\ \Delta V_n\\ \Delta W_n\end{Bmatrix} + \sum_{n=1}^{13} N_n M_{1n} [V_n] \begin{Bmatrix}\Delta\alpha_n\\ \Delta\beta_n\end{Bmatrix} \tag{1}$$

where N and $\bar{N}$ are the in-plane quadratic and cubic shape functions, respectively. M_{1n} is the linear shape function which approximates the through thickness displacements. The above shape functions are presented by Koziey and Mirza.[19] The matrix $[V_n]$ is given by v_{1n} and v_{2n} as $[V_n] = [v_{1n}, -v_{2n}]$ where the unit vectors v_{1n} and v_{2n} are directed along the x'- and y'-axis, respectively, and are orthogonal to the unit vector v_{3n} at the nth node. The procedure for construction of the orthogonal basis (v_{1n}, v_{2n}, v_{3n}) is also given by Koziey and Mirza.[19]

In a subsequent study done by El Damatty *et al.*[18] the mass matrix for the consistent shell element $[M_s]$ has been derived and incorporated with the linear stiffness matrix $[K_0]$, derived by Koziey and Mirza,[19] to perform free vibration analysis of shell structures by solving the following equation:

$$([K_0] - \omega^2 [M_s])\{q\} = \{0\} \tag{2}$$

The non-trivial solution equation (2) exists if the determinant of the coefficients vanishes, i.e.

$$|[K_0] - \omega^2[M_s]| = 0 \tag{3}$$

This is solved to obtain the natural frequencies ω_n of the shell and the mode shape $\{q_n\}$. Moreover, in the same study the element formulation has been extended to non-linear behaviour by deriving the non-linear stiffness matrices $[K_L]$ (sum of the linear and the initial strain stiffness matrix) and $[K_S]$ (initial stress stiffness matrix) and the unbalanced load vector $[F]$. The above matrices simulate the effect of large displacements as well as an isotropic strain hardening behaviour of metals based on the Von-Mises yield criteria. These matrices have been also incorporated with the consistent mass matrix to perform non-linear dynamic analysis by solving the following incremental equations of motion:

$$[M_s]\{\ddot{U}^t\} + [C]\{\dot{U}^t\} + [K_L^{t(k-1)} + K_S^{t(k-1)}]\{\Delta U\} = \{R^t\} - \{F^{t(k-1)}\} \tag{4}$$

where $[C]$ is the viscous damping matrix, $\{R\}$ is the external load vector, $\{\Delta U\}$ is the solution of the kth iteration at time t. In the above equation the superscript t denotes variables evaluated at the equilibrium solution at time t; meanwhile the variables which have a superscript $t(k-1)$ correspond to the $(k-1)$th iteration at the time t. The implicit time integration of equation (4) is performed using Newmark's method (see Reference 20) with the implicitness parameters known as $\delta(=0{\cdot}5)$ and $\alpha(=0{\cdot}25)$. Iterations are performed using the Newton–Raphson method within each time step Δt, until equilibrium is reached.

It should be noted that before a global assembly is performed the order of the above square matrices ($[K_L]$, $[K_S]$, $[C]$, $[M_S]$) for one element is 65×65, meanwhile the order of the load vectors ($\{R\}$ and $\{F\}$) is 65×1. However, these vectors and matrices include many zero terms which correspond to the inactive degrees of freedom. Also in the same study,[18] both the free vibration and non-linear time history analyses were verified by conducting analyses of different plate and shell problems and comparing the obtained results to the numerical and experimental results available in the literature. In all examples the element has shown superior performance. For a detailed description of the non-linear dynamic formulation of the consistent shell element together with verifications for the accuracy of the formulation the reader is referred to Reference 18.

3. HYDRODYNAMIC PRESSURE DUE TO SEISMIC EXCITATION

Hydrodynamic pressure develops inside a liquid-filled tank when it is subjected to seismic excitation and acts as a dynamic force on its walls. The dynamic pressure P_d which results from an earthquake motion can be viewed as the sum of two components $P_s + P_I$, where P_s is the long period component (convective) due to sloshing at the free surface of the fluid and P_I is the implusive fluid pressure which varies in phase with the vibrations of the tank walls.

Previous studies concerning seismic analysis of liquid-filled cylindrical tanks indicate that the fundamental sloshing frequencies are much lower than those of the vibrating walls of the shell. These investigations indicated that the vibration of the walls of the tanks are mainly affected by the impulsive component and the sloshing component has no significant effect on these vibrations. The fundamental sloshing frequency ω_s can be described by the following relation:[6]

$$\omega_s^2 = \frac{1{\cdot}84g}{R} \tan \frac{1{\cdot}84H}{R}$$

where g is the acceleration due to gravity, H is the height of the water and R is the radius of the cylindrical tank. It is clear from the above equation that the broader the tank (small H/R ratio) the lower the fundamental sloshing frequency becomes. Due to the inclination of the walls of conical tanks, such structures can be viewed as having a relatively small H/R ratio. As such, the authors would expect that the fundamental

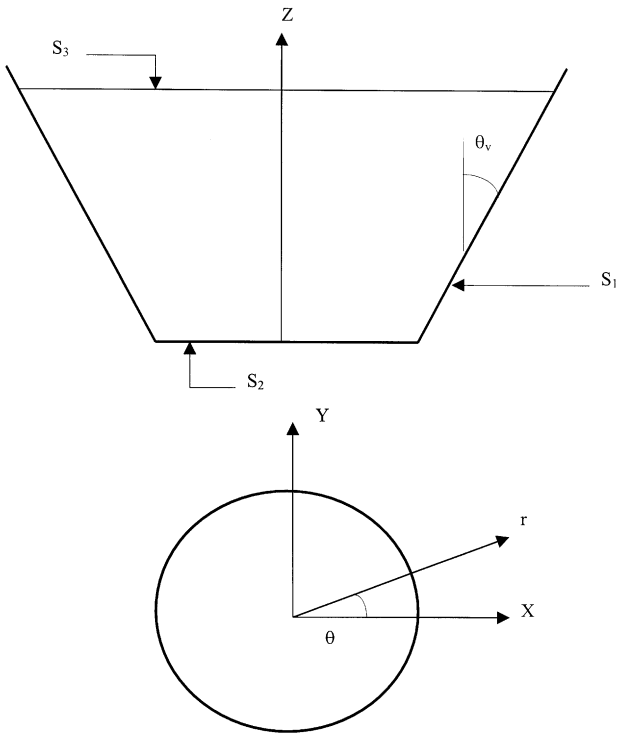

Figure 3. Co-ordinate system for the hydrodynamic pressure formulation

sloshing frequency of conical tanks would be relatively low and that the decoupling between the low-frequency sloshing modes and the high-frequency vibration modes can be still a valid assumption. However, this assumption needs further verification and hence it is planned to be investigated in subsequent studies. Based on the above argument, only the impulsive component of the hydrodynamic pressure P_I is considered. The fluid inside the tank is assumed to be inviscid, incompressible and irrotational, i.e. an ideal fluid. In addition, the base of an elevated conical vessel usually rests on a rigid diaphragm. Assuming that this base is restricted from rocking, the displacements and consequently the accelerations will be identical at all points on the base at a prescribed time t.

In view of the assumptions above, the hydrodynamic pressure P_d resulting from vibrations of a flexible conical vessel filled with water (see Figure 3), is governed by the following set of equations and boundary conditions:

$$\nabla^2 P_d(r, \theta, z, t) = 0 \quad \text{inside the fluid volume } \Omega \tag{5}$$

$$\frac{\partial P_d(r, \theta, z, t)}{\partial n} = -\rho_F \ddot{u}(r, \theta, z, t) \cdot n \quad \text{at the surface } S_1 \tag{6}$$

$$P_d = 0 \quad \text{at the surface } S_3 \tag{7}$$

$$\frac{\partial P_d(t)}{\partial n} = -\rho_F \ddot{u}_s(t) \cdot n \quad \text{at the surface } S_2 \tag{8}$$

where P_d is the hydrodynamic pressure exerted in the tank in access to the hydrostatic pressure; $\ddot{u}(r, \theta, z, t)$ is the acceleration vector at any point of the tank's wall, n is the unit vector normal to the surface of the tank,

ρ_F is the fluid density and $\ddot{u}_s(t)$ is the acceleration vector at the base of the vessel. Surfaces S_1, S_2 and S_3 are as shown in Figure 3. The boundary condition given by equation (8) implies that the dynamic pressure at the surface S_2 ($z=0$) does not vary with the co-ordinates r and θ.

It is clear from the set of equations above that the fluid hydrodynamic pressure P_d depends on the acceleration of the walls of the tank. In turn, this pressure acts as a force on the walls of the tank and hence affects the acceleration of the structure. Consequently, a fluid–structure interaction results and has to be considered to obtain a reasonable estimate of the seismic response of liquid-filled tanks.

4. BOUNDARY ELEMENT METHOD FOR HYDRODYNAMIC PRESSURE

The boundary element method was used by Haroun[5] to obtain the hydrodynamic pressure acting on the walls of a cylindrical tank due to a seismic excitation. A similar approach is used here to obtain the hydrodynamic pressure for the case of elevated liquid-filled conical tanks subjected to seismic movement.

The general idea is to interpolate the dynamic pressure using shape functions (modes) which satisfy the partial differential equation governing the initial value problem and also the time-independent boundary conditions as applicable to the problem. The amplitude of each mode is then obtained by satisfying the rest of the time-dependent boundary conditions in an integral sense.

The solution of the partial differential equation given by equation (5) was derived by Haroun,[5] and is presented in Appendix II as a series solution. Considering the terms which satisfy both the free surface boundary condition, given by equation (7), and the condition of constant dynamic pressure at the base resulting from equation (8), the hydrodynamic pressure can be interpolated using the linearly independent functions H_{in} as follows:

$$P_d(r, \theta, z, t) = \sum_{n=0}^{N_2} \sum_{i=1}^{N_1} A_{in}(t)\, H_{in}(r, \theta, z) + B(t)(z-h) \tag{9}$$

Here $A_{in}(t)$ and $B(t)$ are the amplitude functions of time. The shape functions H_{in}, are a combination of Bessel's function and transcendental functions (Appendix I), and are given as

$$H_{in}(r, \theta, z) = I_n(\alpha_i r)\cos(\alpha_i z)\cos(n\theta) \tag{10}$$

where I_n are the modified Bessel's functions of the first kind and the coefficients α_i depend on the height of the fluid in the tank h as

$$\alpha_i = (2i-1)\frac{\pi}{2h} \tag{11}$$

The variational functional J for this initial value problem, decribed by equations (5)–(8), is given by

$$J = \int_{t_1}^{t_2} \left[\frac{1}{2} \int_\Omega (\nabla P_d \cdot \nabla P_d)\, dV + \int_S \rho_F \ddot{u} \cdot n P_d\, dS \right] dt \tag{12}$$

where Ω is the volume of the fluid inside the tank and S is the sum of the surfaces S_1, S_2 and S_3 which are shown in Figure 3.

Green's formula is applied to the first term on the right-hand side of equation (12) to give the following expression:

$$J = \int_{t_1}^{t_2} \left[\frac{1}{2} \left\{ \int_S P_d \frac{\partial P_d}{\partial n}\, dS - \int_\Omega P_d \nabla^2 P_d\, dV \right\} + \int_S \rho_F \ddot{u} \cdot n P_d\, dS \right] dt \tag{13}$$

Since the shape functions and consequently the dynamic pressure P_d, given by equation (9), satisfy equation (5) and the free surface boundary condition in equation (7), the variational functional J can be reduced to the following:

$$J = \int_{t_1}^{t_2} \left[\frac{1}{2} \int_{(S_1+S_2)} P_d \frac{\partial P_d}{\partial n} \, dS + \int_{(S_1+S_2)} \rho_F \ddot{u} \cdot n P_d \, dS \right] dt \tag{14}$$

Equation (9) is substituted into expression (14) to obtain the variational functional as a quadratic equation in amplitudes $A_{in}(t)$ and $B(t)$. The first variation of J is taken for the extremum condition which leads to a satisfaction of the boundary condition on the surfaces S_1 and S_2, given in equation (6) and (8), in an integral sense. This results in a determination of the amplitudes $A_{in}(t)$ and $B(t)$ in terms of the acceleration of the walls of the tank $\ddot{u}(t)$. These amplitudes are then back substituted into equation (9) to obtain the dynamic pressure P_d as a function of the co-ordinates r, θ, z and the acceleration $\ddot{u}(t)$.

Assuming virtual displacements $\{\delta(\Delta u)\}$ and using the consistent shell element to interpolate both the virtual displacements and the accelerations of the walls of the tank, the virtual work done by the hydrodynamic pressure δW can be expressed in the following manner:

$$\delta W = \delta \{\Delta U\}^T [DM] \{\ddot{U}^t\} \tag{15}$$

where [DM] represents a fluid added-mass matrix which results from the fluid hydrodynamic pressure. Its elements include both the interpolation functions used in the consistent shell formulation and the mode shapes employed to interpolate the dynamic pressure in the boundary element formulation.

In the following subsections, the fluid added-masses due to the horizontal and the vertical seismic accelerations acting on the liquid-filled conical tanks are obtained.

4.1. Fluid added mass due to horizontal excitation

Due to horizontal excitation acting on a liquid-filled conical tank prevented from rocking, the base of the tank has no movement in the vertical direction. As a consequence, the boundary condition on surface S_2 is given by

$$\frac{\partial P_d}{\partial n} = 0. \tag{16}$$

To satisfy this boundary condition, the coefficient $B(t)$ given in equation (9) must vanish and hence the hydrodynamic pressure distribution can be simplified to the following:

$$P_d(r, \theta, z, t) = \sum_{n=0}^{N_2} \sum_{i=1}^{N_1} A_{in}(t) \, H_{in}(r, \theta, z) \tag{17}$$

Also, the preliminary analyses have shown that only the $\cos\theta$-type modes are excited due to the horizontal acceleration applied to either a perfect tank or a tank with axisymmetric imperfections. This result agrees with the numerical studies in the literature for liquid-filled cylindrical tanks subjected to horizontal excitation. It should be noted that the $\cos(n\theta)$ modes can be excited for tanks which have non-axisymmetric imperfections. Since this study will be limited to conical tanks which are either perfect or have only axisymmetric imperfections. Since this study will be limited to conical tanks which are either perfect or have only axisymmetric imperfections, the expression for the dynamic pressure can be simplified to the following:

$$P_d(r, \theta, z, t) = \sum_{i=1}^{N_1} A_{i1}(t) \, H_{i1}(r, \theta, z) \tag{18}$$

where

$$H_{i1}(r, \theta, z) = I_1(\alpha_i r) \cos(\alpha_i z) \cos(\theta) \tag{19}$$

Now, the first term on the RHS of equation (14) can be written as

$$\frac{1}{2}\int_{S_1} P_d \frac{\partial P_d}{\partial n}\, ds = \frac{1}{2}\{A_{i1}(t)\}^T_{1\times N_1}[C^*]_{N_1\times N_1}\{A_{i1}(t)\}_{N_1\times 1} \tag{20}$$

where

$$C^*_{ij} = \int_{S_1} H_{i1}\frac{\partial H_{j1}}{\partial n}\, ds. \tag{21}$$

The derivative $\partial H_{j1}/\partial n$ can be evaluated using the chain rule as follows:

$$\frac{\partial H_{j1}}{\partial n} = \frac{\partial H_{j1}}{\partial r}\frac{\partial r}{\partial n} + \frac{\partial H_{j1}}{\partial z}\frac{\partial z}{\partial n} \tag{22}$$

For conical tanks, $(\partial r/\partial n)$ and $(\partial z/\partial n)$ are equal to $(\cos\theta_V)$ and $(-\sin\theta_V)$, respectively, where θ_V is the angle of inclination of the generator of the tank with the vertical. The derivatives $(\partial H_{j1}/\partial r)$ and $(\partial H_{j1}/\partial z)$ can be obtained from equation (19). The derivatives above are substituted into equation (22) which leads to

$$\frac{\partial H_{j1}}{\partial n} = \alpha_i I_1'(\alpha_i r)\cos(\alpha_i z)\cos(\theta)\cos(\theta_V) + \alpha_i I_1(\alpha_i r)\sin(\alpha_i z)\cos(\theta)\sin(\theta_V) \tag{23}$$

Equations (19) and (23) are then substituted into equation (21), and the integration is performed by discretizing the surface S_1 using triangular elements and the Gaussian quadratic scheme for numerical integration to obtain components of the matrix $[C^*]$ which is a symmetric full matrix. It is also pointed out here that 79 Gaussian integration points are used to achieve the numerical integration. This integration order ensures an accurate numerical integration of polynomials of the 20th degree and is found to be sufficient for the discretization employed in the applications presented in the companion paper.[21]

The second integral I on the RHS of equation (14) is given by

$$I = \int_{S_1} \rho_F p_d \ddot{u}\cdot n\, ds \tag{24}$$

The rotatory inertia is neglected and the acceleration $\ddot{u}$ at any point on the surface S_1 is approximated using the cubic interpolation functions $\bar{N}$ of the consistent shell element to give

$$I = \rho_F \sum_{i=1}^{N_1} A_{i1}(t) \sum_{\text{Elem}} \int_{\text{SEL}} H_{i1}(r,\theta,z)\{G^*\}^T_{1\times 39}\, dS\{\ddot{U}^T\}_{39\times 1} \tag{25}$$

where

$$\{G\}^T = \{\bar{N}_1 l_{31}\ \bar{N}_1 l_{32}\ \bar{N}_1 l_{33}\ \ldots\ \bar{N}_{13} l_{31}\ \bar{N}_{13} l_{32}\ \bar{N}_{13} l_{33}\} \tag{26}$$

l_{3i} are the direction cosines of the unit outward normal to the surface; note that Elem is the number of consistent shell elements and SEL is the area of each shell element used to discretize the surface S_1. $\{\ddot{U}^t\}_{39\times 1}$ is the vector which includes the accelerations of the nodal displacements of the shell element (excluding the rotational degrees of freedom) and is given by

$$\{\ddot{U}^t\}^T = \{\ddot{U}^t_1\ \ddot{V}^t_1\ \ddot{W}^t_1\ \ldots\ \ddot{U}^t_{13}\ \ddot{V}^t_{13}\ \ddot{W}^t_{13}\} \tag{27}$$

Substituting equations (20) and (25) into equation (14) and taking the first derivative with respect to the amplitude function $A_{i1}(t)$ gives the following:

$$\{A_{i1}(t)\}_{N_1\times 1} = -\rho_F[C^*]^{-1}_{N_1\times N_1}\sum_{\text{Elem}}[F]_{N_1\times 39}\{\ddot{U}^t\}_{39\times 1} \tag{28}$$

where matrix $[F]_{N_1\times 39}$ is given by

$$[F]_{N_1\times 39}=\begin{bmatrix}\int_{SEL}\bar{N}_1 l_{31}H_{11}\,ds & \int_{SEL}\bar{N}_1 l_{32}H_{11}\,ds & \int_{SEL}\bar{N}_1 l_{33}H_{11}\,ds & \dots & \dots & \dots & \dots\\ \dots & \dots & \dots & \dots & \dots & \dots & \dots\\ \dots & \dots & \dots & \dots & \dots & \dots & \dots\\ \dots & \dots & \dots & \dots & \dots & \dots & \dots\\ \int_{SEL}\bar{N}_1 l_{31}H_{N_1 1}\,ds & \int_{SEL}\bar{N}_1 l_{32}H_{N_1 1}\,ds & \int_{SEL}\bar{N}_1 l_{33}H_{N_1 1}\,ds & \dots & \dots & \dots & \dots\end{bmatrix}$$

$$\begin{bmatrix}\dots & \dots & \dots & \dots & \int_{SEL}\bar{N}_{13} l_{31}H_{11}\,ds & \int_{SEL}\bar{N}_{13} l_{32}H_{11}\,ds & \int_{SEL}\bar{N}_{13} l_{33}H_{11}\,ds\\ \dots & \dots & \dots & \dots & \dots & \dots & \dots\\ \dots & \dots & \dots & \dots & \dots & \dots & \dots\\ \dots & \dots & \dots & \dots & \dots & \dots & \dots\\ \dots & \dots & \dots & \dots & \int_{SEL}\bar{N}_{13} l_{31}H_{N_1 1}\,ds & \int_{SEL}\bar{N}_{13} l_{32}H_{N_1 1}\,ds & \int_{SEL}\bar{N}_{13} l_{33}H_{N_1 1}\,ds\end{bmatrix} \tag{29}$$

The integration of the components of the matrix $[F]$ is also carried out numerically using the 79 Gaussian integration points.

It is important to note that before carrying out the multiplication $[C^*]^{-1}\Sigma[F]$, the matrices $[F]$ of all elements on the surface S_1 have to be assembled into the global matrix $[F_1]$, i.e.

$$[F_1]_{N_1\times M}=\sum_{Elem}[F]_{N_1\times 39} \tag{30}$$

where M is the total number of degrees of freedom due to the shell elements employed to discretize surface S_1.

Let the matrix $[F^*]$ result from performing the multiplication $\rho_F[C^*]^{-1}[F_1]$, i.e.

$$[F^*]_{N_1\times M}=\rho_F[C^*]^{-1}_{N_1\times N_1}[F_1]_{N_1\times M} \tag{31}$$

Then, in view of equations (18), (28) and (31), the hydrodynamic pressure on any point on the surface of the tank is given by

$$P_d(r,\theta,z,t)=-\{H\}^T_{1\times N_1}[F^*]_{N_1\times M}\{\ddot{U}^t_1\}_{M\times 1} \tag{32}$$

where

$$\{H\}^T=\{H_{11}\ \ H_{21}\ \ \dots\ \ H_{N,1}\} \tag{33}$$

and $\{\ddot{U}^t_1\}$ is the global vector which includes the acceleration of all degrees of freedom of the surface (excluding the rotational degrees of freedom). Now the virtual work V_M done by the hydrodynamic pressure can be obtained as follows:

$$V_M=\sum_{Elem}\int_{SEL}P_d(r,\theta,z,t)\sum_{i=1}^{13}\bar{N}_i\{\delta(\Delta\underline{U})\}\cdot\underline{n}\,ds \tag{34}$$

or

$$V_{\mathrm{M}} = -\sum_{\mathrm{Elem}} \{\delta\Delta U\}^{\mathrm{T}}_{1\times 39} \int_{\mathrm{SEL}} \{G\}_{39\times 1}\{H\}^{\mathrm{T}}_{1\times N_1}[F^*]_{N_1\times M}\,\mathrm{d}s\{\ddot{U}^t_1\}_{M\times 1} \tag{35}$$

where

$$\{\delta(\Delta U)\}^{\mathrm{T}}_{1\times 39} = \{\delta(\Delta U_1)\ \ \delta(\Delta V_1)\ \ \delta(\Delta W_1)\ \ \ldots\ \ \delta(\Delta U_{13})\ \ \delta(\Delta V_{13})\ \ \delta(\Delta W_{13})\} \tag{36}$$

From equation (35), it can be concluded that the fluid added-mass $[\mathrm{DM}]_{\mathrm{H}}$ is given by

$$[\mathrm{DM}]_{\mathrm{H}} = \sum_{\mathrm{Elem}} \int_{\mathrm{SEL}} \{G\}_{39\times 1}\{H\}^{\mathrm{T}}_{1\times N_1}[F^*]_{N_1\times M}\,\mathrm{d}s. \tag{37}$$

After having evaluated $[F^*]_{N_1\times M}$ using equation (31), it is substituted into equation (37). The integration is again carried out numerically using the 79 Gaussian integration points. It is important to note here that the added-mass matrix $[\mathrm{DM}]_{\mathrm{H}}$ can only be obtained globally, and furthermore, it is a fully populated matrix.

4.2. Fluid added mass due to vertical excitation

When a liquid-filled conical tank is subjected to vertical acceleration, the expected motion of the tank and the resulting hydrodynamic pressure are axisymmetric. Accordingly, the dynamic pressure given by equation (9) can be simplified to the following:

$$P_{\mathrm{d}}(r, z, t) = \sum_{i=1}^{N_1} A_{i0}(t)\, H_{i0}(r, z) + B(t)\, H^*(z) \tag{38}$$

Here the shape functions H_{i0} and H^* are given by

$$H_{i0}(r, z) = I_0(\alpha_i r)\cos(\alpha_i z), \qquad H^*(z) = (z - h) \tag{39}$$

where $I_0(\alpha_i r)$ is the modified Bessel's function of the first kind, $\alpha_i = (2i-1)\pi/(2h)$, and h is the height of the fluid inside the tank.

Following the procedure described in Section 4.1, the fluid added-mass matrix $[\mathrm{DM}]_{\mathrm{V}}$ due to vertical acceleration is given by

$$[\mathrm{DM}]_{\mathrm{V}} = \sum_{\mathrm{Elem}} \int_{\mathrm{SEL}} \{G\}_{39\times 1}\{H\}^{\mathrm{T}}_{1\times N_2}[F^*]_{N_2\times M}\,\mathrm{d}s \tag{40}$$

where $N_2 = N_1 + 1$, the vector $\{G\}$ is as given in Equation (26), and Elem is the number of consistent shell elements and SEL is the area of each shell element used to discretize the surfaces S_1 and S_2 (see Figure 3). The vector $\{H\}^{\mathrm{T}}$ and the matrix $[F^*]$ are as follows:

$$\{H\}^{\mathrm{T}}_{1\times N_2} = \{H_{10}\ \ H_{20}\ \ \ldots\ \ H_{N_1 0}\ \ H^*\} \tag{41}$$

where

$$[F^*]_{N_2\times M} = \rho_{\mathrm{F}}[C^*]^{-1}_{N_2\times N_2}[F_1]_{N_2\times M} \tag{42}$$

$$[F_1]_{N_2\times M} = \sum_{\mathrm{Elem}} [F]_{N_2\times 39} \tag{43}$$

and the matrix $[F]$ is of the following form:

$$[F]_{N_2\times 39}=\begin{bmatrix}
\int_{\mathrm{SEL}}\bar{N}_1 l_{31}H_{10}\,\mathrm{d}s & \int_{\mathrm{SEL}}\bar{N}_1 l_{32}H_{10}\,\mathrm{d}s & \int_{\mathrm{SEL}}\bar{N}_1 l_{33}H_{10}\,\mathrm{d}s & \dots & \dots & \dots & \dots \\
\dots & \dots & \dots & \dots & \dots & \dots & \dots \\
\dots & \dots & \dots & \dots & \dots & \dots & \dots \\
\dots & \dots & \dots & \dots & \dots & \dots & \dots \\
\int_{\mathrm{SEL}}\bar{N}_1 l_{31}H_{N_1 0}\,\mathrm{d}s & \int_{\mathrm{SEL}}\bar{N}_1 l_{32}H_{N_1 0}\,\mathrm{d}s & \int_{\mathrm{SEL}}\bar{N}_1 l_{33}H_{N_1 0}\,\mathrm{d}s & \dots & \dots & \dots & \dots \\
\int_{\mathrm{SEL}}\bar{N}_1 l_{31}H^*\,\mathrm{d}s & \int_{\mathrm{SEL}}\bar{N}_1 l_{32}H^*\,\mathrm{d}s & \int_{\mathrm{SEL}}\bar{N}_1 l_{33}H^*\,\mathrm{d}s & \dots & \dots & \dots & \dots
\end{bmatrix}$$

$$\begin{bmatrix}
\dots & \dots & \dots & \dots & \int_{\mathrm{SEL}}\bar{N}_{13} l_{31}H_{10}\,\mathrm{d}s & \int_{\mathrm{SEL}}\bar{N}_{13} l_{32}H_{10}\,\mathrm{d}s & \int_{\mathrm{SEL}}\bar{N}_{13} l_{33}H_{10}\,\mathrm{d}s \\
\dots & \dots & \dots & \dots & \dots & \dots & \dots \\
\dots & \dots & \dots & \dots & \dots & \dots & \dots \\
\dots & \dots & \dots & \dots & \dots & \dots & \dots \\
\dots & \dots & \dots & \dots & \int_{\mathrm{SEL}}\bar{N}_{13} l_{31}H_{N_1 0}\,\mathrm{d}s & \int_{\mathrm{SEL}}\bar{N}_{13} l_{32}H_{N_1 0}\,\mathrm{d}s & \int_{\mathrm{SEL}}\bar{N}_{13} l_{33}H_{N_1 0}\,\mathrm{d}s \\
\dots & \dots & \dots & \dots & \int_{\mathrm{SEL}}\bar{N}_{13} l_{31}H^*\,\mathrm{d}s & \int_{\mathrm{SEL}}\bar{N}_{13} l_{32}H^*\,\mathrm{d}s & \int_{\mathrm{SEL}}\bar{N}_{13} l_{33}H^*\,\mathrm{d}s
\end{bmatrix} \tag{44}$$

The matrix $[C^*]$ is partitioned in the following way:

$$[C^*]_{N_2\times N_2}=\begin{bmatrix}[C^{11}]_{N_1\times N_1} & [C^{12}]_{N_1\times 1}\\ [C^{21}]_{1\times N_1} & [C^{22}]_{1\times 1}\end{bmatrix} \tag{45}$$

where

$$C_{ij}^{11}=\int_S H_{i0}\,\frac{\partial H_{j0}}{\partial n}\,\mathrm{d}s \tag{46}$$

$$C_{ij}^{12}=C_{ji}^{21}=\int_S H_{i0}\,\frac{\partial H^*}{\partial n}\,\mathrm{d}s \tag{47}$$

$$C^{22}=\int_S H^*\,\frac{\partial H^*}{\partial n}\,\mathrm{d}s \tag{48}$$

and, S is the sum of the surfaces S_1 and S_2 shown in Figure 3 with n the unit outward normal to the surface.

The derivatives of the functions H_{i0} and H^* with respect to the normal direction n are obtained by following the same procedure described in Section 4.1 to give

$$\frac{\partial H_{i0}}{\partial n} = \alpha_i I'_0(\alpha_i r)\cos(\alpha_i z)\cos(\theta_v) + \alpha_1 I_0(\alpha_i r)\sin(\alpha_i z)\sin(\theta_v) \tag{49}$$

$$\frac{\partial H^*}{\partial n} = -\sin(\theta_V) \tag{50}$$

where θ_V is the angle of inclination of the generator of the tank with the vertical direction.

Note that when the integration of equations (46)–(48) is carried out over the surface S_2, θ_V is replaced by zero in equations (49) and (50).

In the above formulation, all integrations are carried out numerically, using 79 Gaussian integration points within the triangular elements used to discretize surfaces S_1 and S_2.

It should be mentioned here that the above formulation of both added mass matrices $[DM]_H$ and $[DM]_V$ can be easily modified for any tank which has a different type of shell of revolution by simply using the appropriate expression of the normal derivative of the pressure shape functions instead of applying equations (23), (49) and (50) which are restricted to conical shells.

5. FREE VIBRATION FORMULATION OF LIQUID-SHELL SYSTEM

The natural frequencies ω_n and the corresponding mode shapes $\{q_n\}$ of the liquid-shell system can be obtained by solving equation (2) with the replacement of the structure mass matrix $[M_S]$ by the effective mass matrix $[M]$ of the liquid-shell system. The latter is equal to the sum of the mass matrix of the structure $[M_S]$ and the fluid added-mass matrix [DM] as

$$[M] = [M_S] + [DM]. \tag{51}$$

Now, the fluid added-mass [DM] is either $[DM]_H$ or $[DM]_V$ depending on whether lateral or vertical natural frequencies are sought, respectively.

It should be noted that the free vibration analysis is based on the linear stiffness matrix $[K_0]$ and, as such, it does not take into account the change in the stiffness of the tank due to the effect of both the stresses resulting from the hydrostatic pressure and the geometric imperfections. However, the free vibration results give an insight into the time step which can be used to perform time history analysis. They also provide a guidance in choosing an input ground motion which contains the liquid-filled tank fundamental frequencies in its dominant frequency range.

6. NON-LINEAR STABILITY FORMULATION OF LIQUID-SHELL SYSTEM

The non-linear dynamic equations of motion for a liquid-shell system subjected to both horizontal and vertical components of a ground motion are given by

$$[M]\{\ddot{U}^t\} + [C]\{\dot{U}^t\} + [K_L^{t(k-1)} + K_S^{t(k-1)}]\{\Delta U\} = \{R^t\} - \{F^{t(k-1)}\} - [M]\{H\}a_H^t - [M]\{V\}a_V^t. \tag{52}$$

The effective mass matrix $[M]$ is the sum of the structure's mass and the fluid added-mass matrices due to both the horizontal and vertical accelerations, i.e.

$$[M] = [M_S] + [DM]_H + [DM]_V \tag{53}$$

The sum of the matrices $[K_L + K_S]$ represents the tangential stiffness matrix $[K_{Tan}]$. The damping matrix $[C]$, appearing in equation (4), is obtained using the Rayleigh method as a linear combination of the effective

mass matrix $[M]$ and the tangential stiffness matrix $[K_{\text{Tan}}]$, i.e.

$$[C] = \alpha[M] + \beta[K_{\text{Tan}}] \tag{54}$$

The coefficients α and β are obtained by solving the following equations:

$$\alpha + \beta\omega_1^2 = 2\omega_1\xi_1 \tag{55}$$

$$\alpha + \beta\omega_2^2 = 2\omega_2\xi_2 \tag{56}$$

where ω_1, ξ_1 and ω_2, ξ_2 are the frequencies and the damping ratios for the first and the second mode shapes, respectively, of the liquid-filled tank. Note that in the above formulation for damping, the damping matrix was evaluated based on the tangent stiffness matrix rather than the initial stiffness matrix. This assumption is conservative since it leads to lower damping values when plastification starts to take place in the tank and the tangent stiffness matrix is consequently reduced.

Other terms in equation (52) are the vectors $\{\Delta U\}$, $\{\dot{U}^t\}$ and $\{\ddot{U}^t\}$ which represent the incremental nodal displacements, the total nodal velocities and the total nodal accelerations relative to the ground motion. The load vector $\{R^t\}$ results from the hydrostatic pressure acting on the walls of the tank while the terms a_{H}^t and a_{V}^t are the components of the ground acceleration in the horizontal and vertical directions, respectively, at time t. Finally, the vectors $\{H\}$ and $\{V\}$, which correspond to the consistent shell element, are given by

$$\{H\}_{1\times 65}^T = \{1000010000 \ \ldots \ 10000\} \tag{57}$$

$$\{V\}_{1\times 65}^T = \{0100001000 \ \ldots \ 01000\} \tag{58}$$

As previously mentioned, the implicit time integration of the equation of motion is performed using Newmark's method with the implicitness parameters known as $\delta(=0{\cdot}5)$ and $\alpha(=0{\cdot}25)$. Iterations are performed using the Newton–Raphson method within each time step Δt, until equilibrium is reached. Following the procedure described by Bathe,[20] the incremental solution $\{\Delta U\}$ which corresponds to the kth iteration during the time step Δt, can be obtained by solving the following equation:

$$[K^{*t(k-1)}]\{\Delta U\} = \{R^t\} - \{F^{t(k-1)}\} - [M_{\text{S}}]\{A^{t(k-1)}\} - [C]\{B^{t(k-1)}\} \tag{59}$$

The matrix $[K^{*\text{T}(k-1)}]$ is an effective stiffness matrix of the following form:

$$[K^{*t(k-1)}] = [K_{\text{L}}^{t(k-1)}] + [K_{\text{S}}^{t(k-1)}] + \frac{4}{(\Delta t)^2}[M_{\text{S}}] + \frac{2}{(\Delta t)}[C]. \tag{60}$$

The vectors $\{A^{t(k-1)}\}$ and $\{B^{t(k-1)}\}$ are updated after each iteration during the time step Δt and are obtained by the following:

$$\{A^{t(k-1)}\} = \frac{4}{\Delta t^2}[\{U^{t(k-1)}\} - \{U^{t-\Delta t}\}] - \frac{4}{\Delta t}[\{\dot{U}^{t-\Delta t}\} - \{\ddot{U}^{t-\Delta t}\} \tag{61}$$

$$\{B^{t(K-1)}\} = \frac{2}{\Delta t}[\{U^{t(K-1)}\} - \{U^{t-\Delta t}\}] - \{\dot{U}^{t-\Delta t}\} \tag{62}$$

where $\{U^{t(K-1)}\}$ is the vector which includes the total displacement degrees of freedom after the $(k-1)$ iteration for the current time t; $\{U^{t-\Delta t}\}$, $\{\dot{U}^{t-\Delta t}\}$ and $\{\ddot{U}^{t-\Delta t}\}$ are the vectors of the total nodal displacement, the total nodal velocity and the total nodal acceleration at the equilibrium configuration corresponding to the time $(t-\Delta t)$. Based on the trapezoidal rule, the vectors $\{\dot{U}^{t-\Delta t}\}$ and $\{\ddot{U}^{t-\Delta t}\}$ are evaluated using the

displacements $\{U^{t-2\Delta t}\}$, the velocities $\{\dot{U}^{t-2\Delta t}\}$ and the accelerations $\{\ddot{U}^{t-2\Delta t}\}$ which correspond to the equilibrium solution at the previous time step $(t-2\Delta t)$ as follows:

$$\{\dot{U}^{t-\Delta t}\} = [\{U^{t-\Delta t}\} - \{U^{t-2\Delta t}\}] \frac{2}{\Delta t} - \{\dot{U}^{t-2\Delta t}\} \tag{63}$$

$$\{\ddot{U}^{t-\Delta t}\} = [\{\dot{U}^{t-\Delta t}\} - \{\dot{U}^{t-2\Delta t}\}] \frac{2}{\Delta t} - \{\ddot{U}^{t-2\Delta t}\} \tag{64}$$

The solution of equation (59) proceeds iteratively during the load increment until equilibrium is reached within a specified tolerance. The convergence criterion was based on the energy tolerance which uses the ratio of the work done during the current iteration to the work done during the first iteration. In the above non-linear analysis, the effective stiffness matrix $[K^*]$ is updated at every iteration of the load increments. Localized local bulking or material yielding occurring at the walls of the tank will lead to a reduction of the effective stiffness. The overall buckling of the tank will occur when the effective stiffness matrix vanishes.

7. FREE VIBRATION ANALYSIS OF LIQUID-FILLED CYLINDERS

The natural frequencies of a number of cylindrical tanks which are filled with liquid and subjected to both horizontal and axisymmetric vibrations were determined numerically by Haroun[5] and Haroun and Tayel.[9] The numerical model used by Haroun has been verified by comparison with test results.[5] Since cylindrical tanks can be viewed as special conical vessels having equal top and bottom radii, the boundary integral formulation used for the analysis of liquid-filled conical tanks can be checked by evaluating the fluid added-mass matrices $[DM]_H$ and $[DM]_V$ for the cylinders considered by Haroun using the procedures outlined in Sections 4.1 and 4.2, respectively. These matrices are then incorporated into the eigenvalue analysis as described in Section 5 to evaluate the natural frequencies of such liquid-filled cylinders due to $\cos\theta$ type (horizontal excitation) and axisymmetric (vertical excitation) vibrations. Results of the free vibration analyses are presented in the following subsections.

7.1. Natural frequencies due to horizontal vibration

A cylindrical tank with radius (R) and height (H) equal to 24′ (7·32 m) and 72′ (21·95 m), respectively, is assumed to be filled with water ($\rho_F = 0{\cdot}94 \times 10^{-4}$ lb s^2/in^4, 1000 kg/m^3). The tank is made of steel with $\rho_s = 0{\cdot}733 \times 10^{-3}$ lb s^2/in^4 (7833 kg/m^3), $E = 30 \times 10^6$ lb/in^2 ($2{\cdot}068 \times 10^5$ MPa) and $v = 0{\cdot}3$. Three different values for the thickness (h) of the tank are assumed as given in Table I. The fundamental natural frequencies of the $\cos\theta$-type vibration of the cylinders are obtained by modelling the wall of the tank using the consistent shell element and evaluating the fluid added-mass $[DM]_H$ as given in Section 4.1. The calculated natural frequencies are tabulated in Table I and are compared to the corresponding frequencies given by Haroun.[5] Excellent agreement can be observed, thus verifying the formulation of the added-mass matrix $[DM]_H$.

Table I. Horizontal vibrations for cylindrical tanks ($R = 7{\cdot}32$ m, $H = 21{\cdot}95$ m)

Thickness h (mm)	f (cps), present analysis	f (cps), Reference 5
25·4	5·35	5·31
10·92	3·60	3·56
7·32	3·00	2·93

Table II. Axisymmetric vibrations for cylindrical tanks (Thickness $h = 25{\cdot}4$ mm)

Tank dimensions Radius R (m) Height H (m)	Empty, current study f (cps)	Empty, Reference 9 f (cps)	Full, current study f (cps)	Full, Reference 9 f (cps)
$R = 7{\cdot}32$ $H = 21{\cdot}95$	57·19	57·8	6·92	6·86
$R = 7{\cdot}32$ $H = 14{\cdot}64$	83·58	83·96	10·26	10·11
$R = 18{\cdot}29$ $H = 12{\cdot}19$	44·0	44·41	6·44	6·40

7.2. Natural frequencies of the axisymmetric vibration

Three steel cylindrical tanks of the same material properties described above and having the dimensions given in Table II, are assumed to be filled with water and subjected to an axisymmetric vibration. The steel shells are also modelled using the consistent shell element. Meanwhile, the fluid added-mass resulting from the axisymmetric vibration $[DM]_V$ is evaluated as presented in Section 4.2 and is added to the mass matrix of the shell. The eigenvalue analyses of the liquid-filled cylindrical tanks lead to the fundamental natural frequencies given in Table II. In addition, free vibration analysis results are presented for empty cylindrical tanks. These are compared, once again, to the corresponding values given by Haroun and Tayel.[9] Again, excellent agreement can be observed which therefore verifies the accuracy of the formulation of the added-mass matrix $[DM]_V$. It should be mentioned here that for this particular example, the base of the tank is assumed to be restrained from any vertical motion. This leads to the requirement that the coefficient $B(t)$ in equation (38) must vanish in order to satisfy the condition of zero acceleration normal to the base of the tank.

8. CONCLUSION

In this paper, a numerical model has been developed to perform free vibration analysis and to ascertain the state of dynamic stability of liquid-filled conical tanks through non-linear dynamic analysis. The model consists of a previously formulated consistent shell element with geometric and material non-linearities included. Meanwhile, the boundary element method was used to derive the fluid added-mass matrices which simulate the impulsive dynamic pressure resulting from the effect of both the horizontal and vertical components of a ground motion acting on a conical tank. The boundary element formulation was verified by using the developed procedure to predict the natural frequencies of cylindrical shells, and to compare obtained results to those available in the literature. The excellent agreement obtained for the liquid-filled frequencies together with previous verification of the consistent shell element formulation gives confidence in the accuracy of the finite-boundary element model to study the seismic performance of conical tanks.

APPENDIX I

Notation

a_H^t	horizontal component of the ground acceleration at time t
a_V^t	vertical component of the ground acceleration at time t
$A_{in}(t)$, $B(t)$	amplitude functions of the hydrodynamic pressure

$[C]$	damping matrix
$[DM]$	fluid added-mass matrix
$[DM]_{\mathrm{H}}$	fluid added-mass matrix resulting from the horizontal ground accelerations
$[DM]_{\mathrm{V}}$	fluid added-mass matrix resulting from the vertical ground accelerations
H, R, h	height, the radius and the thickness of the cylindrical tanks
$\{F\}$	unbalanced load vector
$H_{in}(r, \theta, z)$	shape functions of the hydrodynamic pressure
$[K_{\mathrm{L}}]$	sum of the linear and the initial strain stiffness matrices
$[K_0]$	linear stiffness matrix
$[K_{\mathrm{s}}]$	initial stress stiffness matrix
$[K^*]$	effective stiffness matrix
$[K_{\mathrm{Tan}}]$	tangential stiffness matrix
$[M]$	effective mass matrix
$[M_{\mathrm{s}}]$	mass matrix of the shell
$[M_{1n}]$	through thickness interpolation function
N_n, N_n	quadratic and cubic interpolation functions
P_{d}	hydrodynamic pressure
P_{I}	impulsive component of the hydrodynamic pressure
P_{s}	convective component of the hydrodynamic pressure
r, s, t_1	curvilinear co-ordinates
$\{R\}$	external load vector
V_{1n}, V_{2n}, V_{3n}	consistent shell element nodal unit vectors
x, y, z	global Cartesian co-ordinates
x', y', z'	local Cartesian co-ordinates
$\Delta U_n, \Delta V_n, \Delta W_n$	incremental displacement degrees of freedom
$\Delta\alpha_n, \Delta\beta_n$	incremental rotational degree of freedom

APPENDIX II

Solution of the Laplacian equation in cylindrical co-ordinates

The impulsive component of the hydrodynamic pressure P_{d}, developed inside a liquid-filled tank due to seismic excitation is governed by the Laplacian equation, i.e.

$$\nabla^2 P_{\mathrm{d}} = 0 \tag{65}$$

Using the separation of variables technique, the solution of the Laplacian equation in cylindrical co-ordinates (r, θ, z) is given by[5]

$$P_d(r, \theta, z, t) = A_{in}(t)\cos(n\theta)\begin{Bmatrix} J_n(ir)\cosh(iz) \\ J_n(ir)\sinh(iz) \\ r^n z \\ r^n \\ I_n(ir)\cos(iz) \\ I_n(ir)\sin(iz) \end{Bmatrix} \tag{66}$$

where J_n and I_n are the Bessel's and the modified Bessel's functions of order n, respectively; i is a separation constant and n is the circumferential wave number. It should be noted that the terms in the solution to the Laplacian equation, which lead to singularity at $r = 0$, are not present in equation (66).

REFERENCES

1. G. W. Housner, 'Dynamic pressures on accelerated fluid containers', *Bull. Seism. Soc. Am.* **47**, 15–35 (1957).
2. A. S. Veletsos, 'Seismic Effects in Flexible Liquid Storage Tanks', *Proc. 5th World Conf. Earthquake Engng.*, Roma, Italy, 1974, pp. 630–639.
3. T. Balendra, K. K. Ang, P. Paramasivan and S. L. Lee, 'Seismic design of flexible cylindrical liquid storage tanks', *Earthquake Engng. Struct. Dyn.* **10**, 477–496 (1982).
4. D. C. Barton and J. V. Parker, 'Finite element analysis of the seismic response of anchored and unanchored liquid storage tanks', *Earthquake Engng. Struct. Dyn.* **15**, 299–322 (1987).
5. M. A. Haroun, 'Dynamic analyses of liquid storage tanks', *EERL Report No. 80-04*, Earthquake Engineering Research Laboratory Report, California Institute of Technology, Pasadenas, CA, 1980.
6. M. A. Haroun and G. W. Hou*J*sner, 'Seismic design of liquid storage tanks', *J. Tech. Councils ASCE* **107** (**TC1**), 191–207 (1981).
7. M. A. Haroun and H. M. Ellaithy, 'Model for flexible tanks undergoing rocking', *J. Engng. Mech. ASCE* **III**, 143–157 (1985).
8. M. A. Haroun and M. A. Tayel, 'Axisymmetrical vibrations of tanks — analytical', *J. Engng. Mech. Div. ASCE* **III**, 346–358 (1985).
9. M. A. Haroun and M. A. Tayel, 'Axisymmetrical vibrations of tanks — numerical', *J. Engng. Mech. Div. ASCE* **III**, 329–345 (1985).
10. W. K. Liu and R. A. Uras, 'Transient failure analysis of liquid-filled shells, Part I: theory', *Nucl. Engng. Des.* **117**, 107–140 (1989).
11. W. K. Liu and R. A. Uras, 'Transient failure analysis of liquid-filled shells, Part II: applications', *Nucl. Engng. Des.* **117**, 141–157 (1989).
12. R. A. Uras and W. K. Liu, 'Dynamic Stability Characteristics of Liquid-Filled Shells', *Earthquake Engng. Struct. Dyn.* **18**, 1219–1231 (1989).
13. R. A. Uras and W. K. Liu, 'Dynamic buckling of liquid-filled shells under horizontal excitation', *J. Sound Vib.* **141**, 389–408 (1990).
14. K. Tsukimori, W. K. Liu and R. A. Uras, 'Formulation of dynamic stability of fluid-filled shells', *Nucl. Engng. Des. J.* **142**, 267–297 (1993).
15. K. Tsukimori, W. K. Liu, Y. H. Tsao and R. A. Uras, 'Dynamic stability characteristics of fluid-filled shells under multiple excitations', *Nucl. Engng. Des. J.* **142**, 299–318 (1993).
16. M. Zhou, S. Zheng and W. Zhang, 'Study on elephant-foot buckling of broad liquid storage tanks by nonlinear theory of shells', *Comput. Struct.* **44**, 783–788 (1992).
17. A. A. El Damatty, F. A. Mirza and R. M. Korol, 'Stability of imperfect steel conical tanks under hydrostatic loading', *J. Struct. Engng.* ASCE **123**, 703–712.
18. A. A. El Damatty, R. M. Korol and F. A. Mirza, 'Large displacement extension of consistent shell element for static and dynamic analysis', *Comput. Struct.* **62**, 943–960 (1997).
19. B. Koziey and F. A. Mirza, 'Consistent thick shell element', *Comput. Struct.*, March (1997).
20. K. J. Bathe, *Finite Element Procedures in Engineering Analysis*, Prentice-Hall, Englewood Cliffs, NJ, 1982.
21. A. A. El Damatty, F. A. Mirza and R. M. Korol, 'Stability of elevated liquid-filled conical tanks under seismic loading, Part II — Applications', *Earthquake Engng. Struct. Dyn.* **26**, 1209–1229 (1997).

